Monthly Notices
of the
ROYAL ASTRONOMICAL SOCIETY

MNRAS **475,** 1633–1645 (2018)
Advance Access publication 2017 December 20

doi:10.1093/mnras/stx3275

A photometric study of globular clusters observed by the APOGEE survey

Szabolcs Mészáros,[1★†] D. A. García-Hernández,[2,3] Santi Cassisi,[4] Matteo Monelli,[3†] László Szigeti,[1] Flavia Dell'Agli,[2,3] Alíz Derekas,[1,5] Thomas Masseron,[2,3] Matthew Shetrone,[6] Peter Stetson[7] and Olga Zamora[2,3]

[1]*Gothard Astrophysical Observatory, ELTE Eötvös Loránd University, Szombathely 9707, Hungary*
[2]*Instituto de Astrofísica de Canarias (IAC), E-38205 La Laguna, Tenerife, Spain*
[3]*Departamento de Astrofísica, Universidad de La Laguna, E-38206 La Laguna, Tenerife, Spain*
[4]*INAF-Osservatorio Astronomico di Teramo, via M. Maggini, I-64100 Teramo, Italy*
[5]*Konkoly Observatory, MTA CSFK, Konkoly Thege Miklós út 15-17, H-1121 Budapest, Hungary*
[6]*McDonald Observatory, University of Texas at Austin, Fort Davis, TX 79734, USA*
[7]*Herzberg Astronomy and Astrophysics, National Research Council Canada, 5071 West Saanich Road, Victoria, BC V9E 2E7, Canada*

Accepted 2017 December 15. Received 2017 December 14; in original form 2017 September 22

ABSTRACT

In this paper, we describe the photometric and spectroscopic properties of multiple populations in seven northern globular clusters. In this study, we employ precise ground-based photometry from the private collection of Stetson, space photometry from the *Hubble Space Telescope* (*HST*), literature abundances of Na and O, and Apache Point Observatory Galactic Evolution Experiment (APOGEE) survey abundances for Mg, Al, C, and N. Multiple populations are identified by their position in the $C_{U,B,I}-V$pseudo colour–magnitude diagram (pseudo-CMD) and confirmed with their chemical composition determined using abundances. We confirm the expectation from previous studies that the red giant branches (RGBs) in all seven clusters are split and the different branches have different chemical compositions. The Mg–Al anti-correlations were well explored by the APOGEE and *Gaia*-ESO surveys for most globular clusters, some clusters showing bimodal distributions, while others continuous distributions. Even though the structure (i.e. bimodal versus continuous) of Mg–Al can greatly vary, the Al-rich and Al-poor populations do not seem to have very different photometric properties, agreeing with theoretical calculations. There is no one-to-one correspondence between the Mg–Al anticorrelation shape (bimodal versus continuous) and the structure of the RGB seen in the *HST* pseudo-CMDs, with the *HST* photometric information usually implying more complex formation/evolution histories than the spectroscopic ones. We report on finding two second-generation horizontal branch (HB) stars in M5, and five second-generation asymptotic giant branch (AGB) stars in M92, which is the most metal-poor cluster to date in which second-generation AGB stars have been observed.

Key words: stars: abundances – stars: AGB and post-AGB – globular clusters: general.

1 INTRODUCTION

Multiple populations in globular clusters (GCs) are well known today. They are extensively studied in the literature using both photometric and spectroscopic data. To date, almost all GCs were found to have multiple main sequences (MS) and/or subgiant and/or giant branches (e.g. Piotto et al. 2007, 2015; Milone et al. 2008), which are accompanied by variations in the content of He and light elements, and a small age difference between the distinct substellar populations (D'Antona et al. 2005; Cassisi et al. 2008), except in ω Cen (Marino et al. 2012). For most clusters, the C N O content in GCs is fairly constant to within 0.3 dex (Smith et al. 1996; Ivans et al. 1999; Carretta et al. 2005), and only a handful of clusters have been found where this is not the case, like N1851 (Yong et al. 2009), ω Cen (Marino et al. 2012), M22 (Alves-Brito et al. 2012), and M2 (Lardo et al. 2012, 2013). The formation and evolution of GCs turned out to be a more complex problem than previously thought (Kraft 1994; Gratton, Carretta & Bragaglia 2012), and no individual model is capable of fully explaining the evolution of these objects (see e.g. Renzini et al. 2015, for a review).

Multiple photometric surveys have had the goal to characterize GCs to understand their formation and evolution. The *Hubble Space*

★ E-mail: meszi@gothard.hu
† Premium Postdoctoral Fellow of the Hungarian Academy of Sciences.

Telescope (*HST*) Treasury Project (Piotto et al. 2015; Soto et al. 2017) provides the largest and most precise homogeneous photometric data set of photometry in five filters for 47 GCs. The SUMO project (Monelli et al. 2013) is a ground-based, homogeneous, photometric study of multiple stellar populations in the largest sample of GCs.

The different populations in each cluster have different chemical compositions, which mostly manifest in light element variations (O, Na, C, N, Mg, and Al) along the red giant branch (RGB). These elements are known to (anti)correlate with each other, and are the result of high-temperature H-burning. The most well-studied anticorrelations are Na–O and Al–Mg. The most extensive study of the southern GCs was carried out by Carretta et al. (2009a,b,c), who focused on the Na–O and Al–Mg anticorrelations. They showed that while these anticorrelations are unique to GCs, the structure or shape of the anticorrelation patterns and spread of abundances depend on the total mass and metallicity of the clusters.

For the northern clusters, the largest homogeneous study was presented by Mészáros et al. (2015) based on data from the Apache Point Observatory Galactic Evolution Experiment (APOGEE; Majewski et al. 2017) part of the 3rd Sloan Digital Sky Survey (SDSS-III; Eisenstein et al. 2011). APOGEE was a high-resolution near-infrared survey focused on the *H* band (15 090–16 990 Å; Wilson et al. 2012), and observed more than 100 000 red giant stars from all components of the Milky Way. The survey lasted from 2011 to 2014, and its successor, APOGEE-2, will continue until 2020. Mészáros et al. (2015) were able to conduct a more detailed analysis of the Mg–Al anticorrelation, because more stars with higher Al abundances were observed than in previous studies. This allowed the discovery of significantly different shapes in Mg–Al anticorrelation between clusters. Analysis of the CO and CN lines in the *H* band made it possible to measure [C/Fe] and [N/Fe] abundance ratios for most stars, revealing the C–N anticorrelation in the whole sample of investigated clusters; however, the measurement error of these abundances was relatively high. For the southern clusters, the most recent examination of Mg and Al was carried out by Pancino et al. (2017). They used *Gaia*-ESO DR4 data to explore the Mg–Al anticorrelation in nine clusters and found extended anticorrelations in only the more metal-poor clusters.

Combining photometry with abundances is a powerful tool in understanding GC formation/evolution (Monelli et al. 2013) and it was fundamental in discovering second-generation asymptotic giant branch (SG-AGB) stars in GCs. The lack of SG-AGB stars in GCs puzzled astronomers in recent years. Campbell et al. (2013) did not find Na-rich AGB stars in NGC 6752, which is the main tracer element of SG stars in GCs. The possible lack of SG-AGB stars presented a challenge for stellar evolution models and the formation of GCs (Charbonnel 2013; Cassisi et al. 2014). Cassisi et al. (2014) argued that the lack of SG-AGB stars in NGC 6752 is not consistent with star counts along the horizontal branch (HB) and AGB as well as with the canonical stellar models. Early evidence showing the contrary view came from photometry of NGC 2808 by Milone et al. (2015b), who observed three different populations along the AGB. Later, Johnson et al. (2015) found Na-rich AGB stars in the metal-rich GC 47 Tuc (see also Lapenna et al. 2014). Finally, García-Hernández et al. (2015) definitely solved the apparent tension between observations and models by showing clear evidence of the presence of 14 SG-AGB stars in four different metal-poor ([Fe/H] < -1.0) clusters (M13, M5, M3, and M2). This discovery was based upon using Al as a tracer instead of Na to identify SG stars. As found by Mészáros et al. (2015), deriving [Al/Fe] from the atomic lines of Al in the *H* band can be clearly used to separate SG stars from first generation. Later SG-AGB stars were also found in M4 (Lardo et al. 2017; Marino et al. 2017), NGC 6752 (Lapenna et al. 2016), and NGC 2808 (Marino et al. 2017).

In this paper, we focus on combining the large abundance data set available from the literature with ground-based and *HST* photometry in order to study the differences in the photometric properties of clusters with bimodal and continuous Mg–Al anticorrelations. In addition, we report the first discovery of SG-AGB stars in M92; the most metal-poor cluster in which such stars have been observed.

2 LINKING SPECTROSCOPY WITH PHOTOMETRY

The ground-based *U*, *B*, *V*, *R*, *I* photometry was taken from the private collection of Peter Stetson and is precise to the level of <0.002 mag in the *U* band and to <0.001 mag for the other bands (Stetson et al. 2014).

Photometric and APOGEE data are currently available for seven northern GCs. The advantage of APOGEE data is that all abundances were derived consistently, which allows us a more accurate direct comparison between clusters. Abundances of Fe, Mg, and Al were derived using neutral atomic lines, which were believed to be less affected by non-local thermodynamic equilibrium (NLTE) effects than lines in the optical, because they are formed deeper in the atmosphere. However, it was shown recently that this is not the case, as corrections larger than 0.1 dex may be needed for both Mg (Zhang et al. 2017) and Al (Nordlander & Lind 2017). The O abundances were derived from OH lines, then with the O abundances held constant the [C/Fe] ratios were determined from the CO lines. The final step in the process was to determine [N/Fe] from CN. The Na lines in the *H* band are too weak for any measurements below [M/H] < -0.7 dex; thus, Mészáros et al. (2015) were unable to study the Na–O anticorrelation, even though O measurements were available.

In order to extend our study to the Na–O anticorrelation, we collected abundances of both elements from the literature (see Table 1 for a full list of references). The sample was limited to studies which sampled significant part of the RGB with many stars observed, so only two clusters are discussed in detail, M13 and M5. Carretta et al. (2009a) obtained the largest set of Na and O abundances for the most clusters to date, and discussed M5 in detail. The spectra were acquired with Fibre Large Array Multi Element Spectrograph (FLAMES) mounted on the Very Large Telescope (VLT), and they used the forbidden O lines at 6300.3 and 6363.8 Å, and the Na doublets at 5672−88 and at 6154−60 Å. Both Ivans et al. (2001) and Lai et al. (2011) used the same lines to derive Na abundances, but Ivans et al. (2001) determined the O abundance from the O triplet lines at 7770 Å. All studies carried out the usual NLTE corrections from Gratton et al. (1999).

Na and O abundances for a large number of stars in M13 were extensively studied by Johnson & Pilachowski (2012) and Sneden et al. (2004). Johnson & Pilachowski (2012) did not apply corrections for NLTE effects, while Sneden et al. (2004) applied the correction using the suggested procedure by Gratton et al. (1999).

We matched stars with abundance information from the literature based on their Two Micron All-Sky Survey (2MASS) coordinates with the RA, DEC found in the Stetson data base. Because APOGEE is only able to observe the brightest stars, we limited the search to $V < 16$. For the majority of our targets, the match was easily achievable, but we did not include those stars in our analysis for which the positional differences were larger than 1 arcsec. This resulted only in a handful of rejections and their exclusion has a minimal impact

Table 1. Properties of the studied clusters.

ID	Name	N^a	[Fe/H]^b	Literature^c	Shape^d
NGC 7078	M15	23	− 2.28	a, b, c, d	Bimodal/continuous
NGC 6241	M92	47	− 2.23	n, o	Bimodal/continuous
NGC 5024	M53	15	− 1.95	d	Bimodal
NGC 6205	M13	81	− 1.50	d, e, f, g, h	Continuous
NGC 7089	M2	18	− 1.49	d	Bimodal/continuous
NGC 5272	M3	55	− 1.40	d, i, j, k, l	Bimodal
NGC 5904	M5	121	− 1.24	a, d, j, k, l, m	Continuous

Notes: [a] N is the number of stars analysed in this paper.
[b][Fe/H] reference: Mészáros et al. (2015).
[c]Literature abundances: (a) Carretta et al. (2009a), (b) Sneden et al. (1997), (c) Sobeck et al. (2011), (d) Mészáros et al. (2015), (e) Johnson & Pilachowski (2012), (f) Cohen & Meléndez (2005), (g) Kraft et al. (1992), (h) Sneden et al. (2004), (i) Cavallo & Nagar (2000), (j) Sneden et al. (1992), (k) Ivans et al. (2001), (l) Lai et al. (2011), (m) Ramírez & Cohen (2003), (n) Sneden, Pilachowski & Kraft (2000), (o) Roederer & Sneden (2011).
[d]The shape of Mg–Al anticorrelation from Mészáros et al. (2015).

Table 2. Ground-based photometry and abundances from APOGEE.

2MASS ID	Cluster ID	Phot. ID	U	B	V	R	I	$T_{\rm eff}$	log g	[Fe/H]	[C/Fe]	[N/Fe]	[O/Fe]	[Mg/Fe]	[Al/Fe]	[Si/Fe]	[Ca/Fe]	[Ti/Fe]
2M21301565+1208229	M15	73829	15.492	15.123	14.116	99.999	12.919	4836	1.56	−2.12	9999	9999	9999	0.16	− 0.06	0.35	0.19	9999
2M21301606+1213342	M15	74154	15.635	15.378	14.408	99.999	13.239	4870	1.64	−2.31	9999	9999	9999	0.1	0.57	0.46	0.53	9999
2M21304412+1211226	M15	85742	15.384	14.765	13.635	99.999	12.343	4715	1.28	−2.12	9999	9999	9999	− 0.45	0.63	0.6	0.35	9999
2M21290843+1209118	M15	5875	15.188	14.599	13.504	99.999	12.226	4607	1.03	−2.07	9999	9999	9999	− 0.11	0.75	0.41	9999	9999
2M21294979+1211058	M15	28871	15.246	14.338	13.098	99.999	11.648	4375	0.56	−2.31	−0.44	0.95	0.44	0.17	0.64	0.44	0.06	9999

Note: This table is available online in its entirety in a machine-readable form as supplementary material. A portion is shown here for guidance regarding its form and content. Photometry is from the collection of Peter Stetson, and the abundances are from Mészáros et al. (2015).

Table 3. Photometry and Na and O abundances from the literature.

2MASS ID	U	B	V	R	I	[Fe/H]	[O/Fe]	[Na/Fe]	Literature
2M21295311+1212310	15.276	14.871	13.826	99.999	12.611	−2.306	0.323	0.204	a
2M21295492+1213225	15.032	14.166	12.863	99.999	11.433	−2.225	0.540	− 0.072	a
2M21294359+1215473	15.520	15.282	14.313	99.999	13.157	−2.335	0.278	0.041	a
2M21291235+1210498	15.293	14.694	13.567	99.999	12.283	−2.303	− 0.092	0.703	a
2M21294693+1208265	15.877	15.751	14.892	99.999	13.758	−2.351	0.660	0.003	a

Note: This table is available online in its entirety in a machine-readable form as supplementary material. A portion is shown here for guidance regarding its form and content. Photometry is from the collection of Peter Stetson, and the abundance literature sources are listed in Table 1.

on our science results. The GC M2 is the only *Gaia*-ESO cluster (Pancino et al. 2017) in common with APOGEE. Table 1 lists all (even the ones not discussed in detail) literature sources that were used to collect abundances of Na and O, while abundances of C, N, Mg, and Al were only taken from Mészáros et al. (2015). The photometric magnitudes of stars and their abundances of C, N, Mg, and Al are listed in Table 2, while other literature abundances of Na and O are listed in Table 3.

3 SG -AGB STARS IN M92

As mentioned in the Introduction section, SG-AGB stars had been found in many GCs, except for the most metal-poor clusters, those below [Fe/H] < -2. Here, we use the same technique first employed by García-Hernández et al. (2015), and report on the discovery of SG-AGB stars in one of the most metal-poor GCs, M92, extending the covered metallicity range of observed GCs with SG-AGB stars down to [Fe/H] $= -2.23$.

By combining ground-based photometry with Al abundances from Mészáros et al. (2015), we were able to expand the sample of SG-AGB stars by identifying 10 AGB stars in M92, five of them FG and five SG. Fig. 1 shows three different colour–magnitude diagrams (CMDs) of M92: $U-(U-I)$, $I-(U-I)$, and $V-(B-I)$. AGB stars generally separate most from the RGB stars in the $U-(U-I)$ CMD, and we used this CMD to identify AGB stars. Table 4 lists the AGB stars sampled in M92. Additional validation of these stars being SG ones could be done by examining their O abundances (as all SG stars are O poor); all of our SG-AGB stars are, however, hotter than 4500 K, which made it impossible to measure their [O/Fe] values.

With the discovery of SG-AGB stars in M92, the number of clusters with evidence of multiple populations along the AGB rises to six. Since M92 is one of the most metal-poor clusters in the Galaxy, the presence of SG-AGB stars in this GC provides sound evidence of the fact that these stars are commonly present in all GCs regardless of the cluster properties such as its mass and metallicity. As pointed out by García-Hernández et al. (2015), the lack of previous evidence for SG-AGB stars was – at least partially – due to the use of less precise optical-band photometry, which did not allow a reliable separation of AGB and RGB stars. Another possibility is that NLTE effects in AGB stars are larger than in RGB stars, which results in higher Na abundances, so only using Na to separate SG-AGB stars from FG stars may be misleading. The

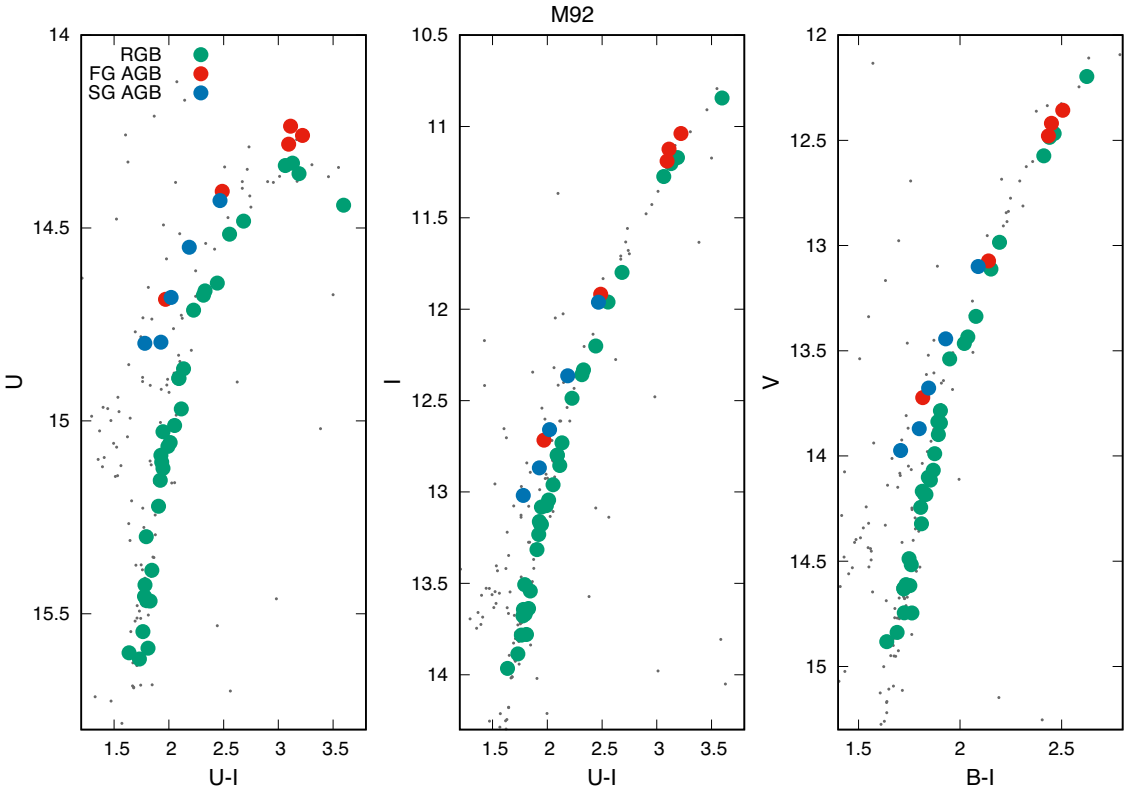

Figure 1. FG(red dots) and SG (blue dots) AGB stars identified by their positions in the $U-(U-I)$, $I-(U-I)$, and $V-(B-I)$ diagrams. Regular RGB stars that have spectroscopic information from Mészáros et al. (2015) are denoted by green circles.

Table 4. Photometry and abundances information of AGBs in M92.

2MASS ID	U	B	V	R	I	$T_{\rm eff}$	log g	[Fe/H]	[C/Fe]	[N/Fe]	[O/Fe]	[Mg/Fe]	[Al/Fe]
						FG stars							
2M17165738+4307236	14.283	13.624	12.479	11.841	11.189	4518	0.84	−2.17	−0.26	0.90	0.68	0.37	−0.19
2M17171342+4308305	14.236	13.574	12.419	11.779	11.124	4504	0.80	−2.23	−0.51	0.51	0.66	0.42	−0.12
2M17171043+4311076	14.260	13.544	12.357	11.699	11.039	4410	0.57	−2.30	−0.57	1.09	0.67	0.33	−0.20
2M17163772+4308411	14.685	14.532	13.723	13.233	12.716	4974	1.87	−2.17	–	–	–	0.16	−0.37
2M17171654+4310449	14.405	14.058	13.073	12.509	11.918	4648	1.14	−2.38	–	–	–	0.41	−0.29
						SG stars							
2M17170588+4310171	14.429	14.051	13.100	12.548	11.962	4729	1.31	−2.26	–	–	–	0.25	0.68
2M17170033+4311478	14.796	14.667	13.870	13.382	12.868	5007	1.95	−2.35	–	–	–	0.34	0.83
2M17170538+4309100	14.799	14.726	13.974	13.503	13.019	4830	1.53	−2.38	–	–	–	0.06	0.73
2M17163427+4307363	14.680	14.504	13.677	13.166	12.659	4864	1.61	−2.10	–	–	–	0.10	0.25
2M17172157+4307408	14.550	14.293	13.443	12.926	12.364	4868	1.61	−2.37	–	–	–	0.21	1.11

adoption of Al abundances from the APOGEE survey may circumvent this problem, although the effect of NLTE on Al lines in the *H* band is still under investigation (Nordlander & Lind 2017) and will become available in future APOGEE data releases. Nevertheless, the combination of multiple abundances known to vary between multiple populations (Na, Al, N) with photometric data is the most accurate way to identify SG-AGB stars.

4 RESULTS BASED ON GROUND-BASED PHOTOMETRY

The first detailed theoretical investigation of the impact of the peculiar chemical patterns of multiple stellar populations on the stellar spectral energy distribution was performed by Sbordone et al. (2011). They found that CNO element abundance variations do affect the stellar spectra essentially at wavelengths shorter than about 400 nm; i.e. the UV spectral windows. This evidence provided a plain support to the use of UV photometric passbands – and combination of UV and optical bands – to properly trace the presence/properties of multiple stellar populations in GCs. Later, Cassisi et al. (2013) – by using synthetic spectra computed for appropriate light element distributions – showed that the Mg–Al anticorrelation has no impact on the stellar models and isochrones, as opposite to C–N and O–Na.

The $C_{U,B,I}$ =$(U-B)-(B-I)$ photometric index was first introduced by Milone et al. (2013) in 47 Tuc. They observed that a pseudo-CMD based on this index is very sensitive to the composition of stars making the different populations stand out in

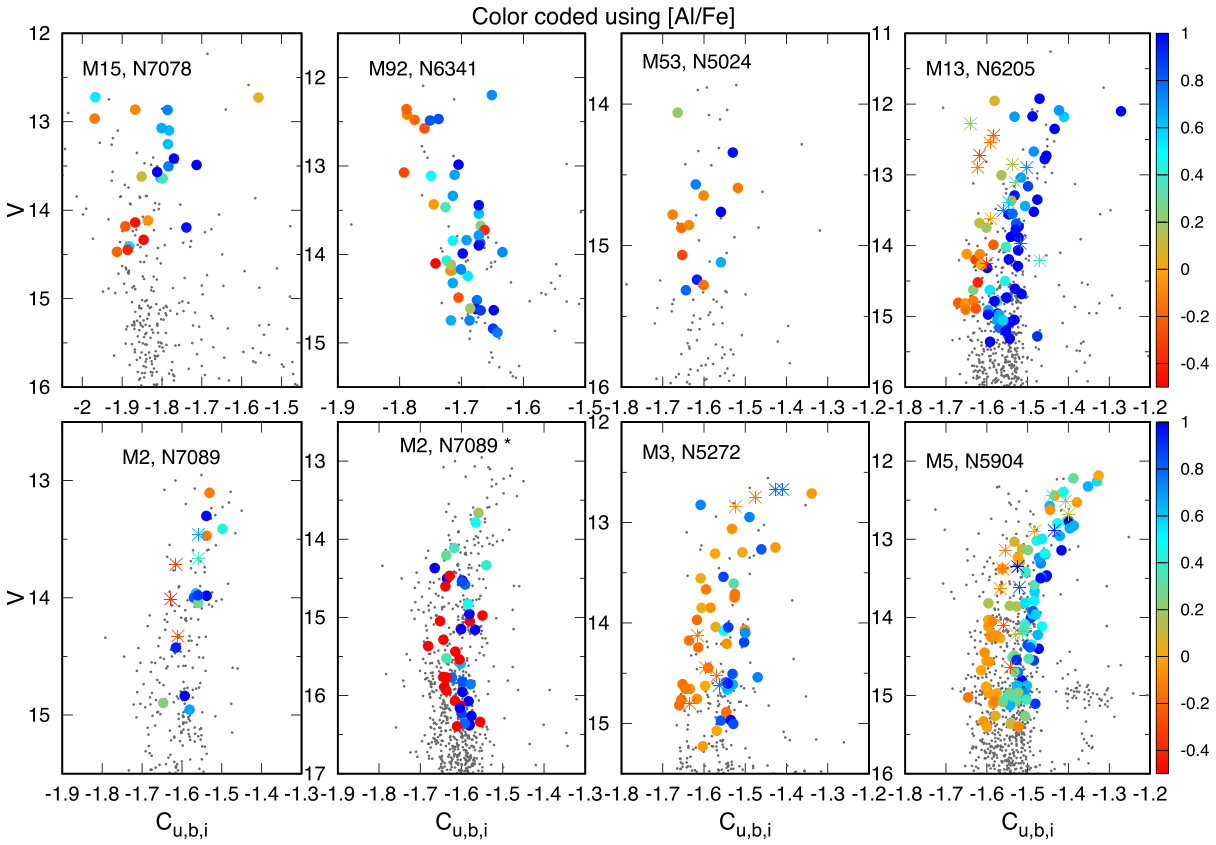

Figure 2. $V - C_{U,B,I}$ diagram colour coded by [Al/Fe]. AGB stars are denoted by stars, and RGB stars are denoted by circles. The second plot of M2 marked by a star shows data from the *Gaia*-ESO survey (Pancino et al. 2017). The more Al-rich SG stars occupy the left side of the RGB, while the more Al-poor FG stars are on the right side of the RGB.

the $C_{U,B,I}$ –V diagram. This is the result of the $C_{U,B,I}$ index being affected by changes in the UV flux caused by variations in [N/Fe]. Elements that correlate with N, like Na and Al, can also be used with the $C_{U,B,I}$ index to identify FG and SG stars, even though none of them has a direct effect on the UV flux.

As Mészáros et al. (2015) noted, some northern clusters show bimodal Al distributions (M53, M3), while other clusters exhibit a continuous distribution (M5, M13). At the same time, we can clearly observe bimodal and/or more continuous RGB branches in both ground-based $C_{U,B,I}$ and *HST* $C_{F275W,F336W,F435W}$ colour indices (see Section 5). Because these colour indices are not directly sensitive to Al variations, we can only explore relationship between abundances and photometry indirectly with the shape of the Mg–Al anticorrelation and the N-induced photometric variations.

Previously, Monelli et al. (2013) were able to systematically study the behaviour of the $C_{U,B,I}$ index in 15 clusters, and they showed that O abundances clearly correlated with the $C_{U,B,I}$ index in most cases. This made it possible to use only ground-based photometry to easily separate first and second population stars in GCs as they are split into two distinct groups in the $C_{U,B,I}$ pseudo-CMD. This technique was also used by Lardo et al. (2017) in M4; Milone et al. (2015a,b) in M2 and NGC 2808; and Nardiello et al. (2015) in NGC 6752, NGC 6397, and M4. Other indices can also be used, like $(U - V) - (V - I)$, but none of them are as sensitive to variations of CN molecular bands in the optical as the $C_{U,B,I}$.

Monelli et al. (2013) did not use Al in their study, but because [Na/Fe] and [Al/Fe] correlate with [N/Fe] in the metal-poor clusters below [Fe/H] $= -1$ (see e.g. Mészáros et al. 2015, and references therein), we expect to see a clear separation in both Al and N. Figs 2 and 3 show the pseudo-CMD of all seven clusters; stars with known Al, N, and O abundances are coloured according to their abundance values. In the traditional CMDs, we cannot see the split RGB belonging to first and second populations. However, in the $C_{U,B,I}$ pseudo-CMD, the separation is clearly highlighted when a different colour coding based on the measured Al abundance is adopted. FG stars with low [Al/Fe] content generally have lower $C_{U,B,I}$ index, as can be seen in both the APOGEE and *Gaia*-ESO data (Pancino et al. 2017). Interestingly, the separation becomes less clear at higher luminosities; above $V < 13$, more FG stars are mixed with SG stars, this is particularly noticeable in M53, M2, M3, and M5. This can be explained with the behaviour of the $C_{U,B,I}$ index. The two main RGB branches have very similar $C_{U,B,I}$ values at high luminosities because the part of the UV and optical spectra where the CN bands can be found loses its sensitivity to the variation of the N abundance. By overplotting the AGB stars on the $C_{U,B,I}$ –V diagram (Fig. 2), we find that AGB stars are not well separated from the RGB stars.

Besides studying the behaviour of Al in the $C_{U,B,I}$ –V diagram, we are also able to plot the literature [Na/Fe] and [O/Fe] values used (Fig. 4). As expected from previous studies and from the Al–O and Na–O anticorrelations, both elements can be used to separate FG and SG stars, as reported previously. In M13, as shown in Fig. 4, the various subpopulations are not well separated when using the Al abundances from Johnson & Pilachowski (2012) to trace them. We note that Johnson & Pilachowski (2012) did not account for any NLTE effects when estimating their [Na/Fe]

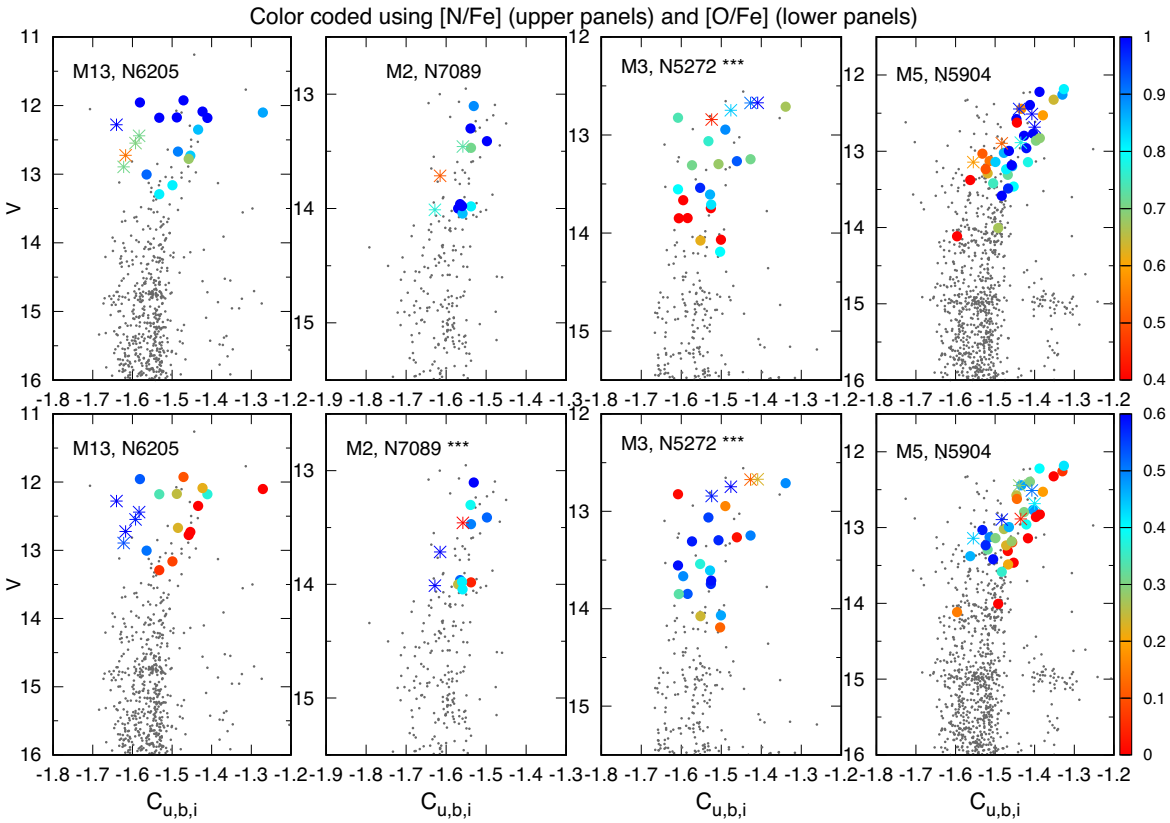

Figure 3. $V - C_{U,B,I}$ diagram colour coded by [N/Fe] and [O/Fe]. AGB stars are denoted by stars, RGB stars are by circles. FG and SG stars divide the RGB similarly to what can be seen in Fig. 2. Clusters with $[M/H] < -1.8$ are not plotted, because the uncertainties of [N/Fe] and [O/Fe] are high (Mészáros et al. 2015).

Table 5. *HST* photometry and abundances from APOGEE.

2MASS ID	Cluster	m_{F275W}	m_{F336W}	m_{F435W}	*HST* ID	[Fe/H]	[C/Fe]	[N/Fe]	[O/Fe]	[Mg/Fe]	[Al/Fe]
2M21295678+1210269	M15	18.381	15.876	14.376	184919	−2.31	−0.36	1.36	0.66	0.34	0.53
2M21300274+1210438	M15	18.353	15.746	14.341	141485	−2.32	–	–	–	0.31	0.74
2M21295666+1209463	M15	18.586	15.842	14.447	104619	−2.27	−0.54	1.25	0.62	0.30	−0.14
2M17170731+4309308	M92	17.075	14.926	14.216	127737	−2.10	–	–	–	0.19	0.48
2M17171342+4308305	M92	17.451	14.860	13.868	76921	−2.23	−0.51	0.51	0.66	0.42	−0.12

Note: This table is available online in its entirety in a machine-readable form as supplementary material. A portion is shown here for guidance regarding its form and content. Photometry is from the *HST* Treasury Project (Piotto et al. 2015; Soto et al. 2017) and the abundances are from Mészáros et al. (2015).

abundances. However, the NLTE correction should amount to 0.1 dex at most (Gratton et al. 1999). So the most plausible explanation for this result is likely due to the lower quality (moderate resolution combined with an extremely short wavelength coverage) spectral data used by Johnson & Pilachowski (2012). This combined with the fact that the RGB sequences converge towards the RGB tip likely explain the apparent problem.

From data in Figs 2–4, it appears evident that the separation along the RGB between FG and SG stars is significant, but not perfect with the most blended cases being those corresponding to M2, M3, and M53. In M92, there is one star with low Al in the SG branch. In M53, there are three stars with high Al values in the FG branch, and in M3 there are at least five stars with low Al in the SG RGB branch. In M2, the *Gaia*-ESO data show three low Al stars in the SG branch, while the separation is clearer in the APOGEE data; however, APOGEE sampled fewer and more luminous stars. We have to note that besides these small differences, both surveys agree very well in terms of identifying FG and SG stars. At present, the explanation of these apparent outlier stars is not clear. Possible reasons are: (1) random errors in the data reduction and/or in the Al abundances spectroscopic determination; and (2) errors in the photometry. The latter is more probable because the *U*-band magnitudes have generally higher errors than other filters, while both APOGEE and *Gaia*-ESO use high-resolution, high S/N spectra and errors up to 1 dex in [Al/Fe] are very unlikely. Finally, it is also possible that the explanation lies in an astrophysical origin, but in order to prove that, a careful examination of all the above possible errors would be necessary, which is beyond the scope of this paper.

5 *HST* PHOTOMETRY IN COMBINATION WITH MG–AL

5.1 Observed properties

Using the preliminary data release of the *HST* Treasury Project (Piotto et al. 2015; Soto et al. 2017), we were able to match stars

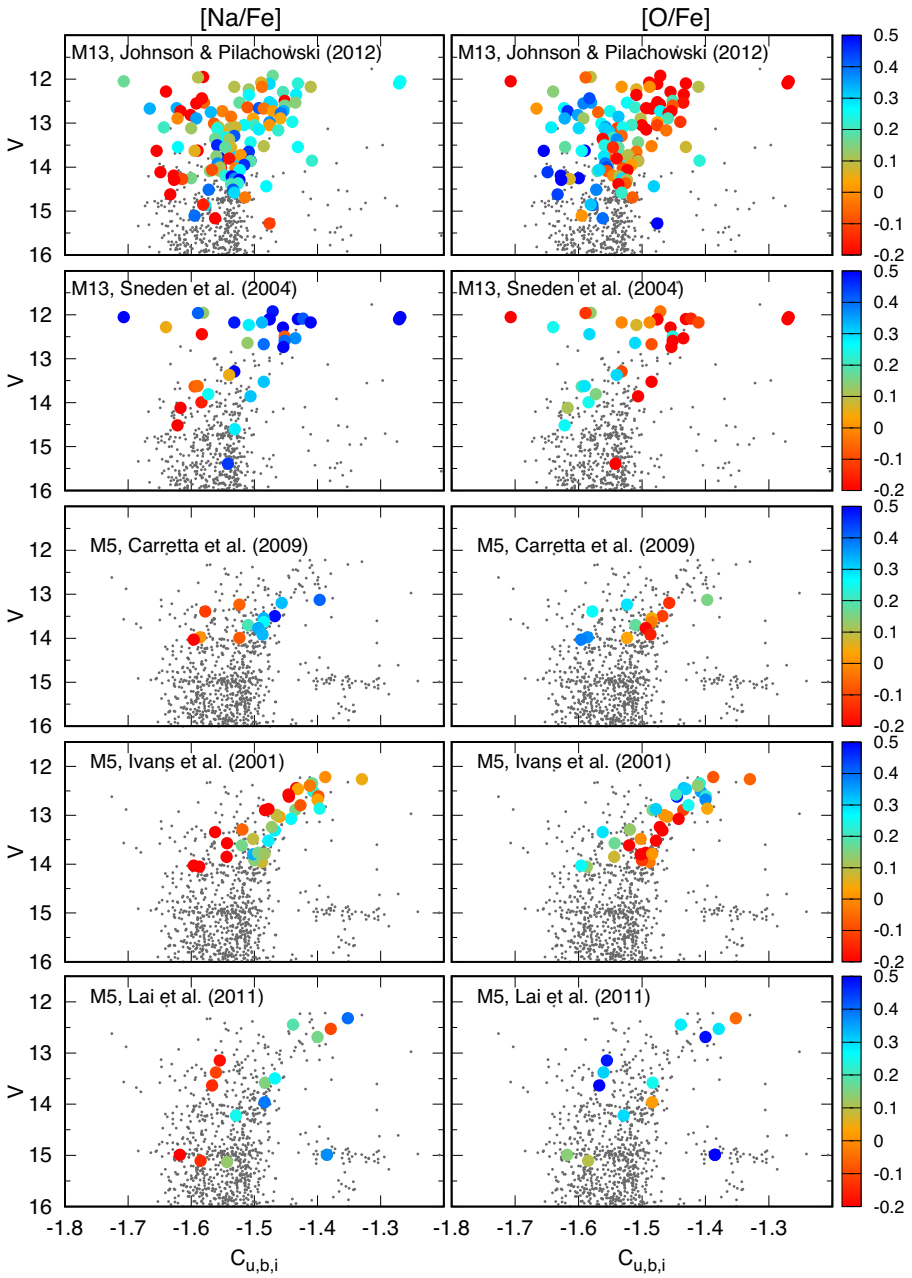

Figure 4. $V - C_{U,B,I}$ diagram colour coding using literature data of [Na/Fe] and [O/Fe]. FG and SG stars are again well separated on the RGB for most clusters.

from Mészáros et al. (2015) with their *HST* catalogue using 2MASS coordinates and a magnitude cut of 18 or 19 in m_{F336W}, depending on clusters to avoid contamination from fainter stars (see Table 5 for the full list of matched stars). The field of view of the *HST* is small compared to that of 2.5-metre SDSS telescope (Gunn et al. 2006) and the *HST* observations focused on the centre of each cluster, while APOGEE observed mostly their outer parts; this resulted in relatively few matches. Altogether, we found 36 stars (four of them AGB stars) in eight clusters in common between APOGEE and *HST*. As can be seen from Fig. 5, the few common stars are usually among the brightest ones near the tip of the RGB, but this still allows us to discriminate between the multiple branches of the RGB due to the high quality of the *HST* photometry and associate these different RGBs with a chemical composition.

This can be done using the $m_{F336W} - C_{F275W,F336W,F435W}$ pseudo-CMD displayed in Fig. 6. This index is a similar diagnostic tool to $C_{U,B,I}$ in that it is also sensitive to the [N/Fe] content of stars and separates multiple populations from each other well. As previously mentioned, one can only use the $C_{U,B,I}$ index to indirectly associate with an Al abundance since the $C_{U,B,I}$ is sensitive to N and not Al directly, and this is also true for the $C_{F275W,F336W,F435W}$ index.

By overplotting the stars with [Al/Fe] abundances from the APOGEE survey, we can conclude from Fig. 6 that Al-rich stars are well separated from the Al-poor ones at the top of the RGB; the SG RGB stars have slightly lower $C_{F275W,F336W,F435W}$ index than FG stars. This is very similar to the behaviour we see when using the $C_{U,B,I}$ index in Fig. 2. From the $C_{U,B,I}$ index, we know that this separation continues down to the turn-off, as shown for 47

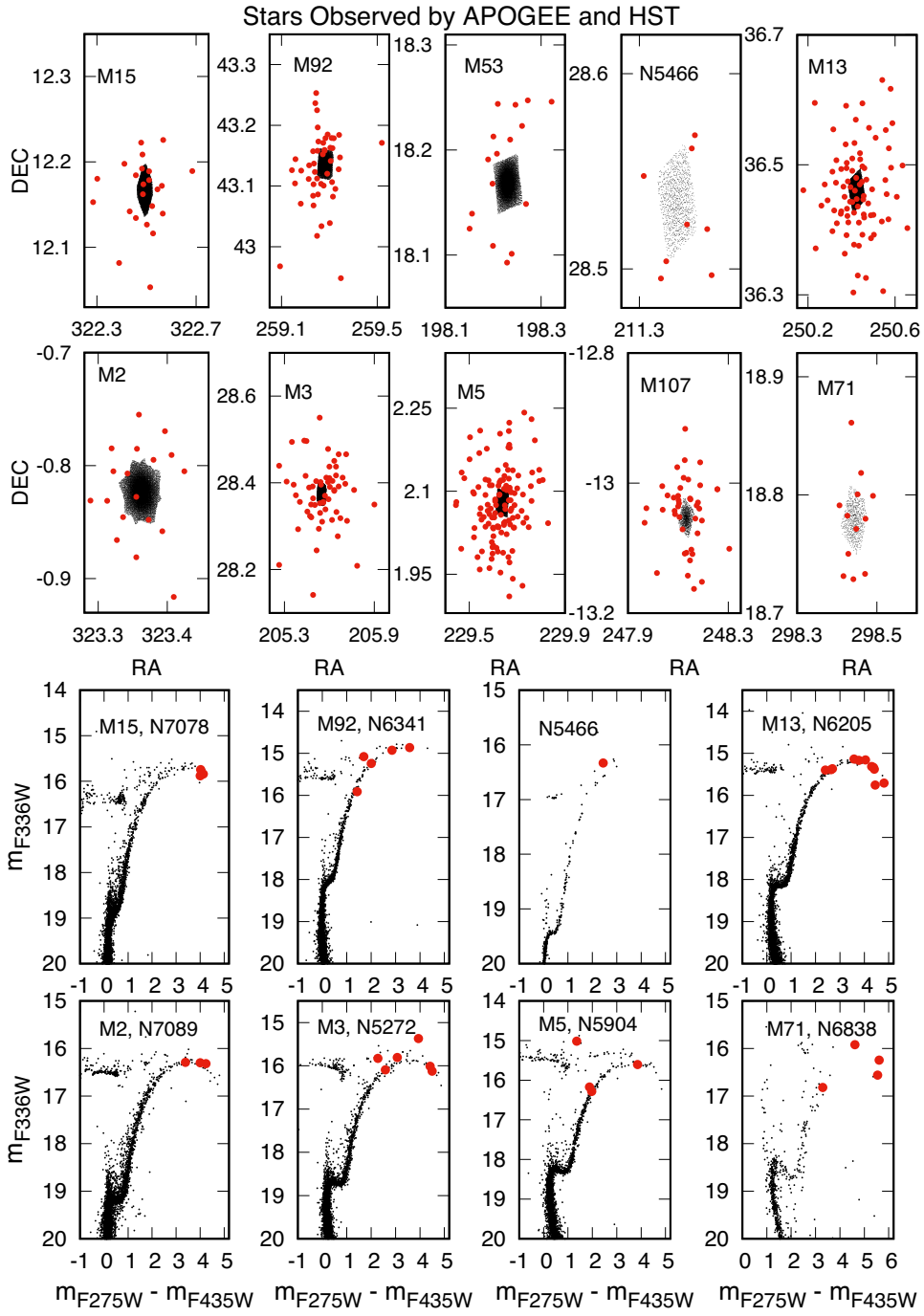

Figure 5. *HST* CMDs (black dots) with stars that are in common with stars observed by the APOGEE survey (red dots). *HST* observes only the centre of each cluster, so the overlap is generally small.

Tuc by Milone et al. (2012) and for NGC 2808 by Milone et al. (2015b). We expect the same to be true for the $C_{F275W,\,F336W,\,F435W}$ index as well, even though we do not have [Al/Fe] available for such low-luminosity stars.

The extremely precise photometry of *HST* allows us to examine any possible correlation in the structure of the RGB, and the shape of the Mg–Al anticorrelation for all 10 GCs in Mészáros et al. (2015). Stellar members from Mészáros et al. (2015) in common with the *HST* photometry are listed in Table 1. The additional three GCs are NGC 5466 ([Fe/H] $= -1.82$), M107 ([Fe/H] $= -1.01$), and M71 ([Fe/H] $= -0.68$). NGC 5466 displays a bimodal Mg–Al anticorrelation, although only eight stars were observed by APOGEE, and only two were SG. The GCs M107 and M71, however, do not display an Mg–Al anticorrelation, as expected from their high metallicities (see below).

In order to investigate possible connection between the photometric and abundance distributions, we contrast the shape of the Mg–Al anticorrelation against the histogram of the number of stars found in the RGB using *HST* magnitudes in M5, M13, M3, and M53 (Fig. 7). M5 and M13 are clear examples of continuous Al distributions, while M3 and M53 are clear examples of bimodal distributions of Al. Other clusters, such as M15, M92, and M2, fall

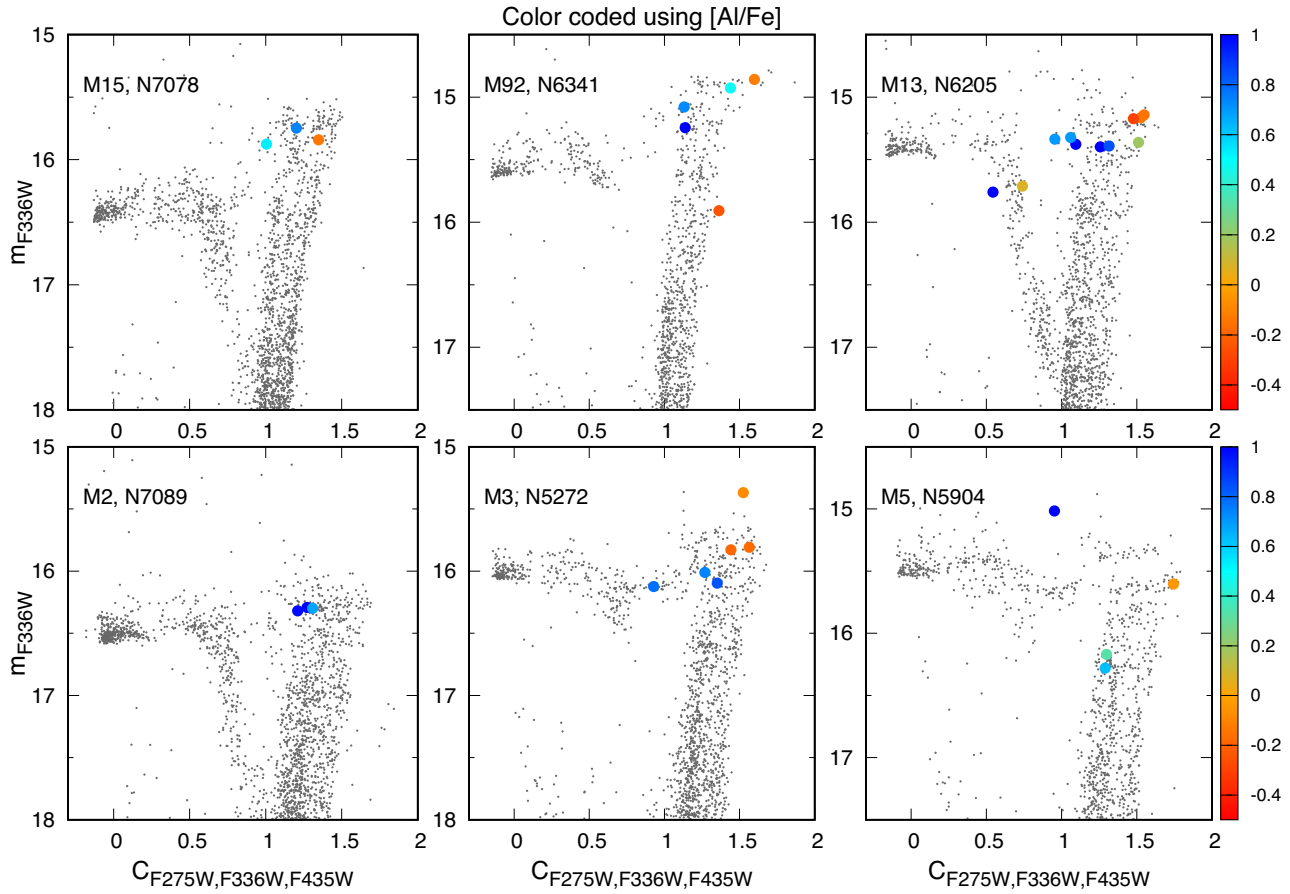

Figure 6. *HST* pseudo-CMDs overplotted by stars in common with APOGEE colour coded by their [Al/Fe]. SG stars with high Al content are on the left branch of the RGB, and FG stars are on the right.

somewhere in between and in order to detect any possible correlation, we chose to show examples of the most extreme distributions. We do this by defining three 0.5-mag-wide regions that are separated by 0.5 mag starting 1.5 mag down from the tip of the RGB and create a histogram of the number of stars found in each of these regions. We conclude from Fig. 7 that there are no visible connection between the shape of the Mg–Al anticorrelation and the histogram of the number of stars found in the RGB. M3 and M53 have very clear distinctive Al-rich and Al-poor populations, while the distributions of the RGB branches are no more distinctive than those of M5 and M13. In fact, M5, which has a continuous Mg–Al distribution, has two distinct peaks in the histogram, while M3 is the opposite. We believe this either rules out a GC formation scenario with two separate star-forming events with no new stars forming in between them, or the time spent between them was not enough the push the two branches of RGBs so far from each other to be visible. Alternatively, the multiple star formation bursts are overlapping. From Fig. 7, one can also confirm that the Al content has no effect on the structure of the $C_{F275W,\,F336W,\,F435W}$ pseudo-CMD, agreeing with the theoretical understanding of Cassisi et al. (2013).

5.2 Possible interpretation of observed properties

In the last decade, several scenarios have been suggested to explain the origin of multiple stellar populations in Galactic GCs, including fast rotating massive stars (Decressin et al. 2007), interacting massive binary stars (de Mink et al. 2009), accretion on circumstellar disc during the pre-MS stage (Bastian et al. 2013; Cassisi & Salaris 2014), supermassive MS stars (Denissenkov & Hartwick 2014), and massive AGB stars (Ventura et al. 2001; D'Ercole et al. 2008). Each one of the proposed scenarios can reproduce some observational evidence; no one of them is able to provide a plain interpretation of the observational framework. All of them have their specific pros and cons (see Renzini et al. 2015, for a detailed discussion on this issue). Even though we are well aware of strong limitation that all mentioned scenarios have, since in this work we focus on the Mg–Al anticorrelation, here we rely on the AGB scenario that (to the best of our knowledge) has been so far the unique one able to provide useful hints on the Al distribution observed in metal-poor ([Fe/H] < -1) GGCs (Ventura et al. 2016). More recently, Dell'Agli et al. (2017) have successfully modelled the Mg–Al anticorrelation in nine GCs observed by APOGEE ($-2.2 <$ [Fe/H] < -0.7) and found remarkable agreement between the observations and theoretical yields from massive AGB stars, supporting the earlier Ventura et al. (2016) results on a smaller APOGEE GCs sample. This further supports the idea that the main driving force of pollution is the ejecta of AGB stars in the range of metallicities considered. For these reasons, we concentrate this discussion on the AGB scenario.

From Fig. 7, we found that in M3 and M53 the separation of multiple RGB branches in the $C_{F275W,\,F336W,\,F435W}$ diagram does not correlate with the discreetness of the Mg–Al anticorrelation. The difference between discrete and continuous Mg–Al distributions

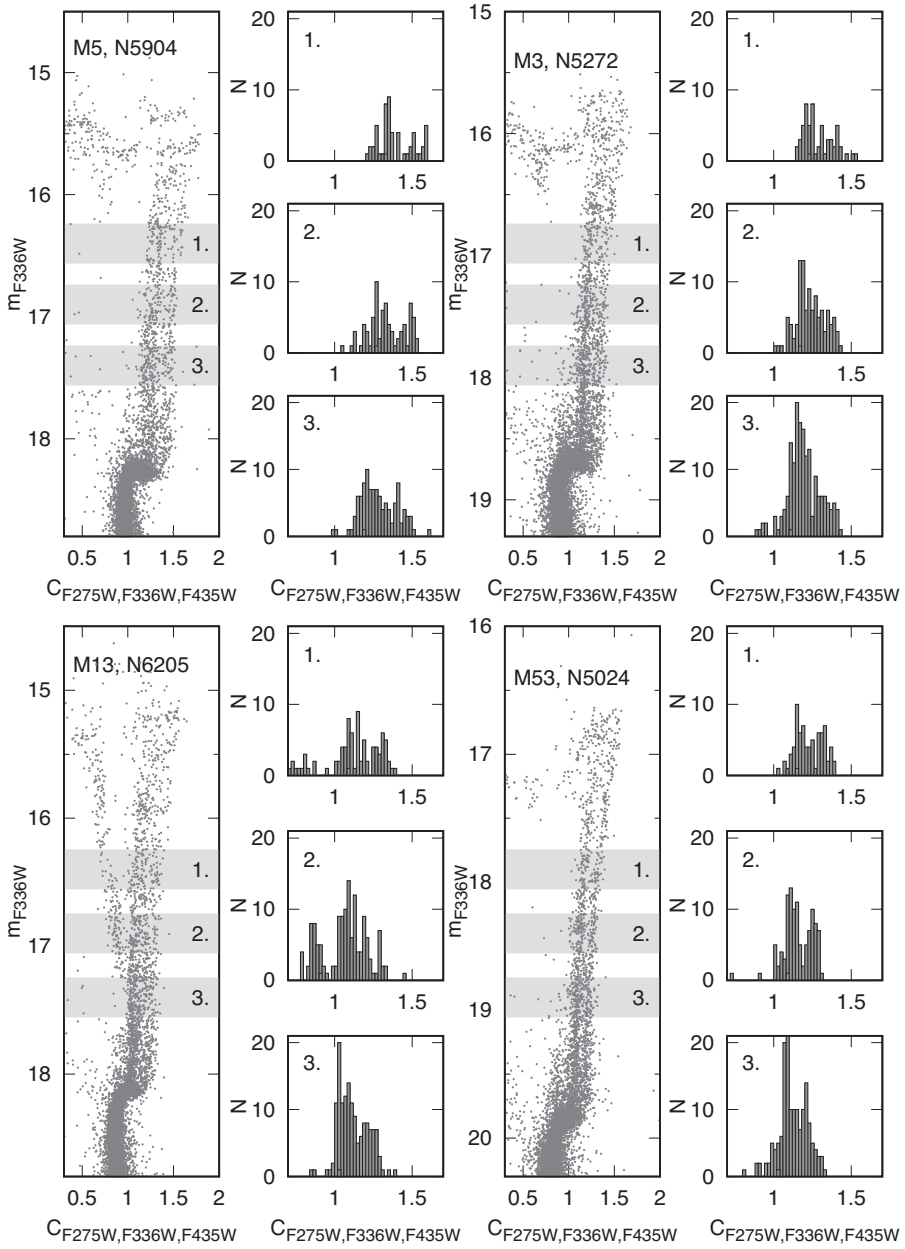

Figure 7. The histograms show the number of stars found in three 0.5-mag-wide regions that are 0.5 mag far from each other starting 1.5 mag down from the tip of the RGB. Clusters with bimodal Al distribution are M3 and M53, continuous distribution are M13 and M5. There is no visible connection between the shape of the Mg–Al anticorrelation and the histogram of the number of stars found in the RGB.

could be explained by the dilution of AGB ejecta with pristine gas; Ventura et al. (2016) found that the Mg–Al anticorrelation can be explained by theoretical yields from massive AGB stars with different dilution levels. According to Ventura et al. (2016), SG stars in M3 formed from gas that contained at least 30 per cent diluted material from FG stars, while there were no stars that formed from 10–30 per cent diluted gas. The situation is different in M13 and M5, two clusters with a continuous distribution of Al abundances, where stars formed from all fractions of dilution, from 0 to 100 per cent. Under the AGB self-enrichment hypothesis, the timing of the return of pristine gas in the central regions of the cluster, after the end of SNe II explosions, is the key factor determining the shape (bimodal versus continuous) of the Mg–Al anticorrelation (D'Ercole, D'Antona & Vesperini 2016).

If the duration of the process is longer than 40–50 Myr, a portion of SG stars form from non-diluted matter, and we thus expect two clear distinct populations, i.e. a bimodal Mg–Al anticorrelation with FG and SG stars showing the initial chemistry and very low-Mg/high-Al, respectively. Conversely, in case of a prompt return of the pristine gas, we then expect a continuous Mg–Al anticorrelation, with different dilution degrees of the AGB ejecta with pristine gas. The main factors affecting the timing of the return of pristine gas are the initial density distribution of the cluster and the number of SNe II explosions, the latter being determined by the total mass of

the cluster. One of the main findings emerging from the study by D'Ercole et al. (2016) is that for a given density distribution the return of the pristine gas takes longer for more massive clusters. This result, in conjunction with the high sensitivity of the degree of the hot bottom burning nucleosynthesis experienced by massive AGBs to the metallicity, provides an explanation of the correlation between the shape of the Mg–Al distribution and the mass and metallicity of the clusters found in recent studies (Carretta et al. 2009a,b,c; Pancino et al. 2017). D'Ercole et al. (2016) clearly demonstrated that the mass of the cluster has a strong effect on the extent of the chemical pollution patterns of the species touched by proton-capture nucleosynthesis. Indeed, the AGB self-enrichment scenario is, so far, the only one that can explain the increasing extension of the Mg–Al anticorrelation (chemical patterns of the chemical elements affected by high-temperature proton capture) observed at lower metallicities (Ventura et al. 2016; Dell'Agli et al. 2017).

If the return of pristine gas is prompt, we then expect a continuous Mg–Al anticorrelation, with different dilution degrees of the AGB ejecta with pristine gas. The *HST* UV pseudo-CMDs are not sensitive to the Al content and we only use Al indirectly through the expected Al–N correlation. In the AGB context, in principle, a clear Mg–Al bimodality should be accompanied by a net separation between N-normal and N-rich stars in the *HST* UV pseudo-CMDs. The CN (and also the CNO) nucleosynthesis, which produces C-poor and N-rich gas, requires lower temperatures than the Mg–Al chain. In AGB stars, N production begins at ∼30 MK, whereas Mg burning demands ∼90–100 M K. This is the reason why N production is expected at all metallicities, while the traces of Mg–Al burning are expected only in low- and intermediate-metallicity ([Fe/H] ≤ -1.0) GCs, as observed (see e.g. Mészáros et al. 2015; Ventura et al. 2016).

In other words, while a net separation in N between FG and SG stars does not necessarily require a clear separation in the Mg–Al plane (as it is still possible that the gas was exposed to CN cycling but not to Mg–Al burning; and this is metallicity dependent), the Al-rich SG stars must have a N content much higher than their FG counterparts. The latter is corroborated by our Fig. 6, which shows that SG Al-rich and FG Al-poor stars lie on the left (N-rich) and right (N-poor) photometric *HST* RGB branches, respectively.

It seems clear that there is no one-to-one correspondence between the Mg–Al anticorrelation shape and the *HST* photometric information such as the appearance of the *HST* pseudo-CMDs, the number and/or shape of RGB branches, and their corresponding chromosome maps, which gives information on the presence of additional FG and/or SG subpopulations (Milone et al. 2017). Both GCs with bimodal (M3 and M53) or continuous (M5 and M13) Mg–Al anticorrelations can display a broad RGB branch with many stars in between the main FG and SG RGB branches, and/or two rather well-defined main FG and SG RGB branches (see Fig. 7). This lack of spectroscopic–photometric correspondence supports previous results that the *HST* photometric information about any single cluster usually gives a more complex star formation history than the spectroscopic one. For example, Milone et al. (2015b) found that NGC 2808 displays three discrete groups in the Mg–Al anticorrelation but five different populations in the *HST* pseudo-CMDs and their corresponding chromosome maps. The presence (or not) of a significant number of stars between the two main branches of the RGB is likely related to the specific formation history of the cluster. Such stars are believed to have intermediate N abundances (as FG is N-poor and SG is N-rich), even if they are slightly Al-rich or not. Stars showing an FG-like chemical pattern but slightly enriched in N are known to be present in other clusters, for example in NGC 2808 (Milone et al. 2015b). D'Antona et al. (2016) identified them as late SG stars formed at ∼90–100 Myr from AGB material strongly diluted with the pristine gas. We note that the occurrence of non-canonical processes – such as extra-mixing during the RGB stage – could also contribute to modify the expected chemical patterns. Finally, it is also possible that the discreetness of the Al distribution is independent of the self-enrichment mechanism, perhaps because the star formation happens in small pockets and it is interrupted by SNe II explosions that clear out most of the gas from the clusters (Bekki, Jerabkova & Kroupa 2017).

Nevertheless, in order to fully understand the connection between Al and N abundances and the $C_{U,B,I}$, and $C_{F275W,F336W,F435W}$ indices, we need N abundances more precise than those of Mészáros et al. (2015). Unfortunately, the available APOGEE N abundance estimates are for the most luminous RGB stars, near the top of the RGB where the separation between the various subpopulations is not very clear. While more precise N measurements will be most certainly published by the APOGEE team, they are still not able to measure the N content of fainter ($H < 12.5$; see Fig. 6) stars in the multiple RGB branches seen by the *HST*.

6 CONCLUSIONS

The combination of photometric magnitudes and chemical information is a powerful tool in understanding the history and evolution of GCs. It was shown by Sbordone et al. (2011) that certain photometric indices sensitive to the abundance of N can be used to study the presence of multiple populations in GCs. Here, we combined these two data sets (photometric and spectroscopic) for seven clusters and examined the behaviour of multiple population of stars in the $C_{U,B,I}$ $-V$ diagram. We found that FG and SG stars are well separated from each other in this diagram, when using elements of Al and N from APOGEE and *Gaia*-ESO. We also found that the separation is less clear at the top of the RGB, because multiple branches converge due to the fact that $C_{U,B,I}$ loses sensitivity because the molecular bands become saturated and insensitive to the variations in N abundance.

We have identified 10 AGB stars in M92, five of them being FG and five are SG. This is the most metal-poor cluster to date in which SG-AGB stars have been found. Combined with García-Hernández et al. (2015), there are now enough clusters containing SG-AGB to conclude that the appearance of SG-AGB is common and does not depend on the cluster's main parameters such as age, luminosity, or metallicity.

We combined the Al abundances from the APOGEE survey with ground-based UBVRI and *HST* photometry and find that clusters with bimodal and continuous Al distributions have similar photometric properties in both data sets. We confirm that Al does not have an effect on the structure of the $C_{U,B,I}$ and $C_{F275W,F336W,F435W}$ pseudo-CMDs, as previously explained by Cassisi et al. (2013). Both GCs with bimodal/discrete (M3 and M53) or continuous (M5 and M13) Mg–Al anticorrelations can display a broad RGB branch. This suggests, under the AGB self-enrichment framework, that the lack of medium Al stars in M3 and M53 is probably the result of stars not forming from 10–30 per cent diluted gas by FG stars.

Because there is no one-to-one correspondence between the Mg–Al anticorrelation shape and the photometric information such as the appearance of the *HST* pseudo-CMDs, both Mg–Al and C–N abundances are needed simultaneously in order to understand the formation history of each cluster and the multiple populations phenomenon. The lack of a spectroscopic–photometric correspondence suggests that the *HST* photometric information usually gives more

complex star formation histories than the spectroscopic one. Since [N/Fe] errors reported by Mészáros et al. (2015) are relatively large (0.12–0.32 dex),[1] more precise CNO abundances, the ability to accurately model CN yields from the internally processed material, and more stars to improve the statistics are definitely needed. Such data may be provided by the on-going APOGEE-2 survey, which will almost triple the number of GC stars observed in the *H* band. The ideal step forward is to get spectroscopic data for the stars observed by the *HST* and the different FG and SG subpopulations seen in the chromosome maps (as already suggested by Milone et al. 2017) but we likely may have to wait for next-generation instruments and/or the big telescopes era for this; because APOGEE, only focusing on bright stars above $H < 12.5$ mag, will not observe the fainter stars down in the RGB that are necessary for a complete analysis.

ACKNOWLEDGEMENTS

We thank the referee for his/her suggestions during the peer-review process, which greatly improved the clarity of the paper. We also would like to thank Paolo Ventura for his useful comments and discussion when preparing this paper.

SzM has been supported by the Premium Postdoctoral Research Program of the Hungarian Academy of Sciences, and by the Hungarian NKFI Grants K-119517 of the Hungarian National Research, Development and Innovation Office. DAGH was funded by the Ramón y Cajal fellowship number RYC−2013 −14182. DAGH, FDA, TM, and OZ acknowledge support provided by the Spanish Ministry of Economy and Competitiveness (MINECO) under grant AYA−2014 −58082-P. SC acknowledges financial support from PRIN-INAF2014. AD has been supported by the ÚNKP-17-4 New National Excellence Program of the Ministry of Human Capacities and the NKFIH K-115709 grant of the Hungarian National Research, Development and Innovation Office. AD and LSz would like to thank the City of Szombathely for support under agreement no. 67.177-21/2016.

Funding for SDSS-III has been provided by the Alfred P. Sloan Foundation, the Participating Institutions, the National Science Foundation, and the US Department of Energy Office of Science. The SDSS-III web site is http://www.sdss3.org/.

SDSS-III is managed by the Astrophysical Research Consortium for the Participating Institutions of the SDSS-III Collaboration including the University of Arizona, the Brazilian Participation Group, Brookhaven National Laboratory, University of Cambridge, Carnegie Mellon University, University of Florida, the French Participation Group, the German Participation Group, Harvard University, the Instituto de Astrofisica de Canarias, the Michigan State/Notre Dame/JINA Participation Group, Johns Hopkins University, Lawrence Berkeley National Laboratory, Max Planck Institute for Astrophysics, New Mexico State University, New York University, Ohio State University, Pennsylvania State University, University of Portsmouth, Princeton University, the Spanish Participation Group, University of Tokyo, University of Utah, Vanderbilt University, University of Virginia, University of Washington, and Yale University.

[1] Note that these errors do not include possible systematic/random effects due to the methodology employed in the chemical abundances derivation; the use of spectral windows versus the entire spectrum, model atmospheres, linelists, etc.

REFERENCES

Alves-Brito A., Yong D., Meléndez J., Vásquez S., Karakas A. I., 2012, A&A, 540, 3
Bastian N., Lamers H. J. G. L. M., de Mink S. E., Longmore S. N., Goodwin S. P., Gieles M., 2013, MNRAS, 436, 2398
Bekki K., Jerabkova T., Kroupa P., 2017, MNRAS, 471, 2242
Campbell S. W. et al., 2013, Nature, 498, 198
Carretta E., Gratton R. G., Lucatello S., Bragaglia A., Bonifacio P., 2005, A&A, 433, 597
Carretta E. et al., 2009a, A&A, 505, 117
Carretta E., Bragaglia A., Gratton R., Lucatello S., 2009b, A&A, 505, 139
Carretta E., Bragaglia A., Gratton R., D'Orazi V., Lucatello S., 2009c, A&A, 508, 695
Cassisi S., Salaris M., 2014, A&A, 563, 10
Cassisi S., Salaris M., Pietrinferni A., Piotto G., Milone A. P., Bedin L. R., Anderson J., 2008, ApJ, 672, L115
Cassisi S., Mucciarelli A., Pietrinferni A., Salaris M., Ferguson J., 2013, A&A, 554, 19
Cassisi S., Salaris M., Pietrinferni A., Vink J. S., Monelli M., 2014, A&A, 571, A81
Cavallo R. M., Nagar N. M., 2000, AJ, 120, 1364
Charbonnel C., Chantereau W., Decressin T., Meynet G., Schaerer D., 2013, A&A, 557, L17
Cohen J. G., Meléndez J., 2005, AJ, 129, 303
D'Antona F., Bellazzini M., Caloi V., Pecci F. F, Galleti S., Rood R. T., 2005, ApJ, 631, 868
D'Antona F., Vesperini E., D'Ercole A., Ventura P., Milone A. P., Marino A. F., Tailo M., 2016, MNRAS, 458, 2122
D'Ercole A., Vesperini E., D'Antona F., McMillan S. L. W., Recchi S., 2008, MNRAS, 391, 825
D'Ercole A., D'Antona F., Vesperini E., 2016, MNRAS, 461, 4088
de Mink S. E., Pols O. R., Langer N., Izzard R. G., 2009, A&A, 507, L1
Decressin T., Meynet G., Charbonnel C., Prantzos N., Ekström S., 2007, A&A, 464, 1029
Dell'Agli F. et al., 2017, MNRAS, (arXiv:1712.04500)
Denissenkov P., Hartwick F. D. A., 2014, MNRAS, 437, L21
Eisenstein D. J. et al., 2011, AJ, 142, 72
García-Hernández D. A., Mészáros S., Monelli M., Cassisi S., Stetson P. B., Zamora O., Shetrone M., Lucatello S., 2015, ApJ, 815, L4
Gratton R. G., Carretta E., Eriksson K., Gustafsson B., 1999, A&A, 350, 955
Gratton R. G., Carretta E., Bragaglia A., 2012, A&AR, 20, 50
Gunn J. E. et al., 2006, AJ, 131, 2332
Ivans I. I., Sneden C., Kraft R. P., Suntzeff N. B., Smith V. V., Langer G. E., Fulbright J. P., 1999, AJ, 118, 1273
Ivans I. I., Kraft R. P., Sneden C. S., Smith G. H., Rich R. M., Shetrone M., 2001, AJ, 122, 1438
Johnson C. I., Pilachowski C. A., 2012, ApJ, 754, L38
Johnson C. I. et al., 2015, AJ, 149, 71
Kraft R. P., 1994, PASP, 106, 553
Kraft R. P., Sneden C., Langer G. E., Prosser C. F., 1992, AJ, 104, 645
Lai D. K., Smith G. H., Bolte M., Johnson J. A., Lucatello S., Kraft R. P., Sneden C., 2011, AJ, 141, 62
Lapenna E., Mucciarelli A., Lanzoni B., Ferraro F. R., Dalessandro E., Origlia L., Massari D., 2014, ApJ, 797, 124
Lapenna E. et al., 2016, ApJ, 826, L1
Lardo C., Pancino E., Mucciarelli A., Milone A. P., 2012, A&A, 548, A107
Lardo C. et al., 2013, MNRAS, 433, 1941
Lardo C., Salaris M., Savino A., Donati P., Stetson P. B., Cassisi S., 2017, MNRAS, 466, 3507
Majewski S. R. et al., 2017, AJ, 154, 94
Marino A. F. et al., 2012, ApJ, 746, 14
Marino A. F. et al., 2017, ApJ, 843, 66
Mészáros S. et al., 2015, AJ, 149, 153
Milone A. P. et al., 2008, ApJ, 673, 241
Milone A. P. et al., 2012, ApJ, 744, 58

Milone A. P., Bedin L. R., Cassisi S., Piotto G., Anderson J., Pietrinferni A., Buonanno R., 2013, A&A, 555, 143
Milone A. P. et al., 2015a, MNRAS, 447, 927
Milone A. P. et al., 2015b, ApJ, 808, 51
Milone A. P. et al., 2017, MNRAS, 464, 3636
Monelli M. et al., 2013, MNRAS, 431, 2126
Nardiello D., Milone A. P., Piotto G., Marino A. F., Bellini A., Cassisi S., 2015, A&A, 573, A70
Nordlander T., Lind K., 2017, A&A, 607, A75
Pancino E. et al., 2017, A&A, 601, 112
Piotto G. et al., 2007, ApJ, 661, L53
Piotto G. et al., 2015, AJ, 149, 91
Ramírez S. V., Cohen J. G., 2003, AJ, 125, 224
Renzini A. et al., 2015, MNRAS, 454, 4197
Roederer I. U., Sneden C., 2011, AJ, 142, 22
Sbordone L., Salaris M., Weiss A., Cassisi S., 2011, A&A, 534, 9
Smith G. H., Shetrone M. D., Bell R. A., Churchill C. W., Briley M. M., 1996, AJ, 112, 1511
Sneden C., Kraft R. P., Prosser C. F., Langer G. E., 1992, AJ, 104, 2121
Sneden C., Kraft R. P., Shetrone M. D., Smith G. H., Langer G. E., Prosser C. F., 1997, AJ, 114, 1964
Sneden C., Pilachowski C. A., Kraft R. P., 2000, AJ, 120, 1351
Sneden C., Kraft R. P., Guhathakurta P., Peterson R. C., Fulbright J. P., 2004, AJ, 127, 2162
Sobeck J. S. et al., 2011, AJ, 141, 175
Soto M. et al., 2017, AJ, 153, 19
Stetson P. B. et al., 2014, PASP, 126, 521
Ventura P., D'Antona F., Mazzitelli I., Gratton R., 2001, ApJ, 550, L65
Ventura P. et al., 2017, ApJ, 831, L17
Wilson J. et al., 2012, Proc. SPIE, 8446, 84460H
Yong D., Grundahl F., D'Antona F., Karakas A. I., Lattanzio J. C., Norris J. E., 2009, ApJ, 685, L62
Zhang J., Shi J., Pan K., Allende Prieto C., Liu C., 2016, ApJ, 833, 137

SUPPORTING INFORMATION

Supplementary data are available at *MNRAS* online.

Table 2. Ground-based photometry and abundances from APOGEE.
Table 3. Photometry and Na and O abundances from the literature.
Table 5. *HST* photometry and abundances from APOGEE.

Please note: Oxford University Press is not responsible for the content or functionality of any supporting materials supplied by the authors. Any queries (other than missing material) should be directed to the corresponding author for the article.

This paper has been typeset from a TEX/LATEX file prepared by the author.